# TWO INDUCTION MOTORS ELECTRIC DRIVE WITH ROTATORY STATOR

**Alexander PUGACHEV**
Electronic, Radioelectronic and Electric Engineering department, Bryansk State Technical University
Bryansk, Russian Federation, Email: alexander-pugachev@rambler.ru

**Andrey KOSMODAMIANSKIY**
Traction Rolling Stock department, Moscow State University of Railway Engineering (MIIT)
Moscow, Russian Federation

***Abstract:*** *The brief survey of techniques to restrict the start current of an induction motor is carried out. The electric drive consisted of two identical induction motors one of which has rotatory stator is proposed as an alternative type of soft-starters. The principle of its operation from the theoretical background is considered. The equivalent circuit of electric drive is developed and mathematical model on its base is designed. The experimental setup to validate the mathematical model is described. The results of both simulation by Matlab and experimental investigation are presented. The assessment of power losses in the proposed electric drive shows a possibility to use it as an adjustable electric drive in some applications without strong requirements to speed control.*

***Key words:*** *induction motor, soft start, rotatory stator, equivalent circuit, power losses*

## 1. Introduction

The survey of state-of-art electric drives shows that there are a number of a different techniques and approaches to control the speed of an induction motor [1, 2, 3]. Mostly, it needs a frequency converter to feed an induction motor and implement some of control schemes that provide desirable quality indicators in terms of efficiency, stability, accuracy, etc. But there are still a quite considerable number of applications that do not have a strict requirements on the wide range of speed, its accuracy, transient time and so on. Instead of it, the restriction of start currents and torques, the ability of work in severe environmental operating conditions have to be fulfilled. The electric drives of this kind are often connected to synchronous generator that provide supplying. The typical examples of such applications are the fans, air compressors, water and oil pumps, forge and press mechanisms designed for quarry, mines, Far North conditions. The spectrum of options of frequency converter are often excessive to cover demands over control of these applications. Moreover, the use of severe duty frequency converter is linked to additional payments to buy it and necessity of high-skilled staff to maintain it throughout its operation. As a result, the most preferable way to avoid the complications is to introduce a technique of soft starting only to restrict start currents and torques [4].

The historically first method for soft start is implementation of one or more sets of resistors which, during start, are connected in series with the grid to the stator winding. There is a very high power dissipation in the resistors, resulting in the requirement for very high power rated resistors. Typically, the resistors will dissipate as much as 150% - 200% the power rating of the motor for the duration of the start. The significant improvement of efficiency during start was reached by substitution of resistors by reactance. It led to considerable reducing of heat losses, but the problem of non-discrete control was still in place.

Another approaches for soft starting are the introducing of auto transformer, the use of star delta starter, slip ring or wound rotor motors with additional resistor connected to it. Each of approaches has some advantages and shortcomings that limit its implication.

Nowadays, the most popular soft starters for an induction motor in the wide range of power are based on thyristor or IGBT schemes [5]. Thyristor or IGBT-based soft starters allow to increase smoothly the voltage applied to the stator winding that lead to respective change of current and torque. As a main deficiency of these devices, the necessity of presence of skilled electronic staff has to be highlighted for maintaining and repairing.

One of feasible ways to solve this problem is to employ the two induction motors electric drive with rotatory stator. This electric drive does not content any semiconductor switches or resistive elements. It has simple scheme for electrical connection and high reliability during operation. The main shortcoming of the drive is some sophistication in mechanical designs. The proposed electric drive are also able to control speed in a small range of it without significant derating of efficiency.

The results of both theoretical and experimental investigation of the electric drive are presented in this article.

## 2. Principle of operation

The scheme of the electric drive consisted of two the same wound rotor induction motors one of which has a rotatory stator is shown in Fig. 1.

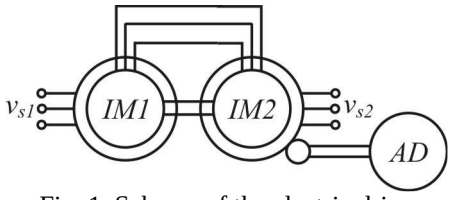


Fig. 1. Scheme of the electric drive

The value of rated power of each induction motor, IM1 and IM2, is the same and it equals to half of rated power needed by electric drive. The stator windings are connected to the same voltage supply, $v_{s1}=v_{s2}$. The rotor windings are connected in series with each other. The shafts of motors are linked together. The stator of the IM2 is mounted so that it can rotate around the axle by some auxiliary device, AD.

The principle of operation is described by Fig. 2.

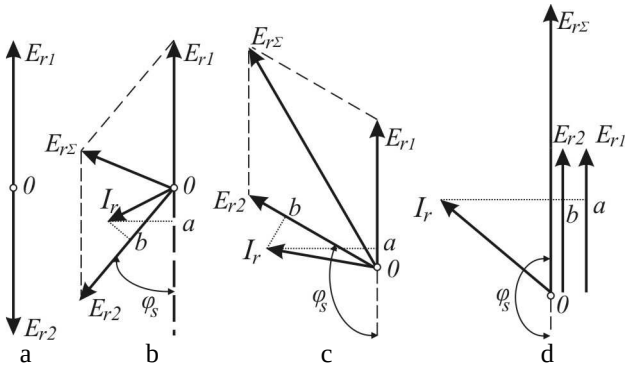


Fig. 2. Vector diagrams of the electric drive

While the electric rotation angle of the IM2 stator $\varphi_s=0$ (Fig. 2,a), the EMFs, $E_{r1}$ and $E_{r2}$, induced in the rotor windings of the IM1 and IM2, respectively, are directed opposite, its resulting value of EMF, $E_{r\Sigma}$, equals to null. It leads to the rotor current of $I_r=0$ and the torque of $T_{e\Sigma}=0$.

If the rotation angle of $\varphi_s\neq0$ (Fig. 2,b), then the $E_{r\Sigma}\neq0$, the current of $I_r$ starts to flow in the rotor windings and $T_{e\Sigma}\neq0$ that lead to the moving of the motors shafts. The active component of $0a$ of the rotor current for the IM1 has an opposite sign to the $E_{r1}$. It means that under this angle of $\varphi_s$ the torque of the IM1 is negative to the resulting torque of two motors and its speed and it has braking effect. The active component of $0b$ of the rotor current for the IM2 has the same sign as the $E_{r2}$ that lead to the positive torque.

Further increasing of the $\varphi_s$ rotates the $E_{r2}$ and, consequently, $E_{r\Sigma}$ clockwise (Fig. 2,c). As a result, the both $Oa$ and $Ob$ are directed the same direction as the respective EMF. The torques of IM1 and IM2 have the same direction as the resulting torque and speed.

If $\varphi_s=\pi$ (Fig. 2,d), $E_{r1}$ and $E_{r2}$ coincide totally and the $E_{r\Sigma}$ equals to algebraic sum of $E_{r1}$ and $E_{r2}$, i.e. $E_{r\Sigma}=E_{r1}+E_{r2}$. The $I_r$ is placed the same way to $E_{r1}$ and $E_{r2}$ and both IM1 and IM2 have the same torques $T_{e1}=T_{e2}=T_{e\Sigma}/2$. Under these conditions the speed of the motors has the maximum value that depends on the voltage supply frequency as in direct on line mode.

## 3. Mathematical model

The six differential equations relating the stator and rotor voltages to the stator and rotor currents has been reduced to four equations by using the famous park transformation [6]. This transformation offers, besides simplification, the advantage to eliminate completely the time varying parameters.

The equivalent circuit for the two induction motors electric drive with rotatory stator in the stationary frame is shown in Fig. 3.

In Fig. 3, $R_s$, $R_r$ denote the stator and rotor resistances; $L_{ls}$, $L_{lr}$ do the stator and rotor leakage inductances; $L_m$ does the magnetizing inductance; $R_{ir}$ does the resistance representing the iron losses in the stator due to eddy curent and to hysteresis current; $\omega_r$, $\omega_s$ do the electric speeds of the both rotor shafts and the stator of IM2; $i_s$, $i_r$ do the currents flowing through the stator and rotor windings; $i_m$, $i_{ir}$ do the currents flowing through the inductance of $L_m$ and resistance of $R_{ir}$; $\lambda_s$, $\lambda_r$, $\lambda_m$ do the stator, rotor and magnetizing flux linkages, respectively. Subscripts of 1 and 2 reffer all the variables and parameters to the IM1 and IM2, respectively.

According to the equivalent circuit, the stator and rotor voltage equations in the stationary frame in the vector form are the follows:

$$v_{s1}=R_s\cdot i_{s1}+\frac{d\lambda_{s1}}{dt}+\frac{d\lambda_{m1}}{dt} \tag{1}$$

$$v_{s2}=R_s\cdot i_{s2}+\frac{d\lambda_{s2}}{dt}+\frac{d\lambda_{m2}}{dt}-j\omega_s(\lambda_{s2}+\lambda_{m2}) \tag{2}$$

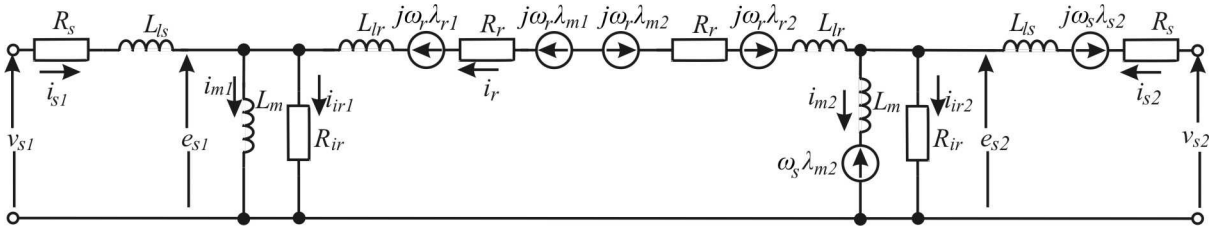


Fig. 3. Equivalent circuit for the two induction motors electric drive with rotatory stator

$$0 = 2R_r \cdot i_r + \frac{d\lambda_{r1}}{dt} + \frac{d\lambda_{r2}}{dt} + \frac{d\lambda_{m1}}{dt} + \frac{d\lambda_{m2}}{dt} - \quad (3)$$
$$- j\omega_r(\lambda_{r1} + \lambda_{m1} + \lambda_{r2} + \lambda_{m2}) - j\omega_s\lambda_{m2}$$

$$R_{ir} \cdot i_{ir1} = \frac{d\lambda_{m1}}{dt} \quad (4)$$

$$R_{ir} \cdot i_{ir2} = \frac{d\lambda_{m2}}{dt} + \omega_s\lambda_{m2} \quad (5)$$

$$i_{m1} + i_{ir1} = i_{s1} + i_{r1} \quad (6)$$

$$i_{m2} + i_{ir2} = i_{s2} + i_{r2} \quad (7)$$

The actual sign of $\lambda_m$ in the equation of (3) depends on the direction of currents flowing through the magnetically coupled inductances and it will be extracted further in this section.

From the section 2 one can conclude that the space position of the two stators is not coincided in general. Since that, it is necessary to introduce two stationary frames linked to respective stators. Letting stationary frame of α1β1 links to the stator of IM1 and stationary frame of α2β2 links to the stator of IM2, we obtain space position of all the winding, as shown in Fig. 4.

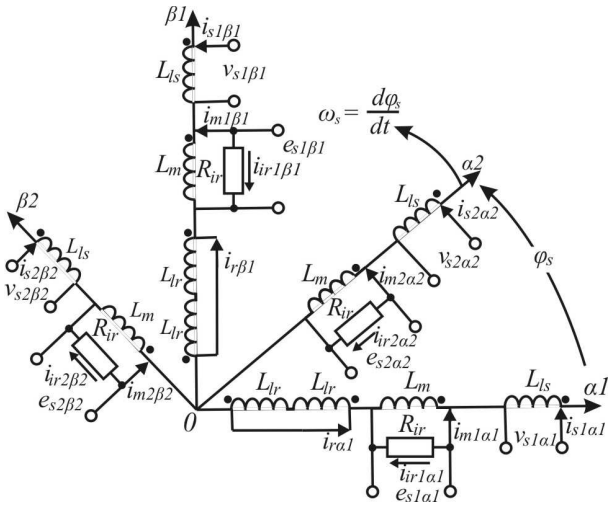

Fig. 4. Space position of the windings

It is obvious that two induction motors have the shared shaft and rotor circuit and do not have any magnetic links. To decide the equations of (1) - (7), it needs to employ the dependance between flux linkages ans respective currents:

$$\lambda_s = L_{ls}i_s \quad (8)$$

$$\lambda_r = L_{lr}i_r \quad (9)$$

$$\lambda_m = L_m i_m \quad (10)$$

Generally, the space position of the windings is changing during electric drive working. The frames has been choosen so that the rotor windings of both IM1 and IM2 (all inductances of $L_{lr}$ in the Fig. 4), the stator winding of the IM1 (inductances of $L_{ls}$ with currents of $i_{s1\alpha1}$ and $i_{s1\beta1}$ flowing through) and the magnetizing winding of the IM1 (inductances of $L_m$ with currents of $i_{m1\alpha1}$ and $i_{m1\beta1}$ flowing through) were aligned to frame of α1β1. Thus, the only windings that rotate with the frame of α2β2, i.e. with the stator of the IM2, are the stator winding of the IM2 (inductances of $L_{ls}$ with currents of $i_{s2\alpha2}$ and $i_{s21\beta2}$ flowing through) and the magnetizing winding of the IM2 (inductances of $L_m$ with currents of $i_{m2\alpha2}$ and $i_{m2\beta2}$ flowing through). The rotor windings connected in series and described by equation of (3) cause the necessity of transforming of the IM2 magnetizing flux linkages from the α2β2 to the α1β1. Since the coordinates of the currents and flux linkages complete the whole range of changing during the electrical angle of $\varphi_s=2\pi$ then the next equations follow with regard to directions of the currents of $i_{r\alpha1}$, $i_{r\beta1}$, $i_{m2\alpha2}$, $i_{m2\beta2}$ flowing through the magnetically coupled inductances of the IM2 and rotation angle shown in the Fig. 4:

$$\lambda_{m2\alpha1} = -\lambda_{m2\alpha2}\cos\varphi_s + \lambda_{m2\beta2}\sin\varphi_s \quad (11)$$

$$\lambda_{m2\beta1} = -\lambda_{m2\alpha2}\sin\varphi_s - \lambda_{m2\beta2}\cos\varphi_s \quad (12)$$

Thus, taking (8) - (12) into account, the equations of (1) - (7) is transformed below to solve it relatively to the 6 unknown currents and 4 flux linkages.

The stator voltages equations:

$$v_{s1\alpha1} = R_s \cdot i_{s1\alpha1} + L_{ls}\frac{di_{s1\alpha1}}{dt} + \frac{d\lambda_{m1\alpha1}}{dt} \quad (13)$$

$$v_{s1\beta1} = R_s \cdot i_{s1\beta1} + L_{ls}\frac{di_{s1\beta1}}{dt} + \frac{d\lambda_{m1\beta1}}{dt} \quad (14)$$

$$v_{s2\alpha2} = R_s \cdot i_{s2\alpha2} + L_{ls}\frac{di_{s2\alpha2}}{dt} + \frac{d\lambda_{m2\alpha2}}{dt} + \quad (15)$$
$$+ \omega_s(L_{ls}i_{s2\beta2} + \lambda_{m2\beta2})$$

$$v_{s2\beta2} = R_s \cdot i_{s2\beta2} + L_{ls}\frac{di_{s2\beta2}}{dt} + \frac{d\lambda_{m2\beta2}}{dt} - \quad (16)$$
$$- \omega_s(L_{ls}i_{s2\alpha2} + \lambda_{m2\alpha2})$$

The rotor voltages equations:

$$0 = 2R_r \cdot i_{r\alpha1} + 2L_{lr}\frac{di_{r\alpha1}}{dt} + \frac{d\lambda_{m1\alpha1}}{dt} - \frac{d\lambda_{m2\alpha2}}{dt} \times$$
$$\times\cos\varphi_s + \frac{d\lambda_{m2\beta2}}{dt}\sin\varphi_s + \omega_r(2L_{lr}i_{r\alpha1} + \lambda_{m1\beta1}) + \quad (17)$$
$$+ (\omega_r + \omega_s)(-\lambda_{m2\alpha2}\sin\varphi_s - \lambda_{m2\beta2}\cos\varphi_s)$$

$$0 = 2R_r \cdot i_{r\beta1} + 2L_{lr}\frac{di_{r\beta1}}{dt} + \frac{d\lambda_{m1\beta1}}{dt} - \frac{d\lambda_{m2\alpha2}}{dt} \times$$
$$\times\sin\varphi_s - \frac{d\lambda_{m2\beta2}}{dt}\cos\varphi_s - \omega_r(2L_{lr}i_{r\alpha1} + \lambda_{m1\alpha1}) - \quad (18)$$
$$- (\omega_r + \omega_s)(-\lambda_{m2\alpha2}\cos\varphi_s + \lambda_{m2\beta2}\sin\varphi_s)$$

The magnetizing and iron losses contour equations:

$$R_{ir} \cdot i_{ir1\alpha1} = \frac{d\lambda_{m1\alpha1}}{dt} \quad (19)$$

$$R_{ir} \cdot i_{ir1\beta1} = \frac{d\lambda_{m1\beta1}}{dt} \quad (20)$$

$$R_{ir} \cdot i_{ir2\alpha2} = \frac{d\lambda_{m2\alpha2}}{dt} + \omega_s \lambda_{m2\alpha2} \quad (21)$$

$$R_{ir} \cdot i_{ir2\beta2} = \frac{d\lambda_{m2\beta2}}{dt} - \omega_s \lambda_{m2\beta2} \quad (22)$$

To omit all the $i_{ir}$ from (19)-(22), it needs to use the current equations. The current equations of the IM1:

$$i_{m1\alpha1} + i_{ir1\alpha1} = i_{s1\alpha1} + i_{r\alpha1} \quad (23)$$

$$i_{m1\beta1} + i_{ir1\beta1} = i_{s1\beta1} + i_{r\beta1} \quad (24)$$

To write current equations of the IM2, it needs to transform the rotor currents from frame of α1β1 to frame of α2β2:

$$i_{r\alpha2} = i_{r\alpha1}\cos\varphi_s + i_{r\beta1}\sin\varphi_s \quad (25)$$

$$i_{r\beta2} = -i_{r\alpha1}\sin\varphi_s + i_{r\beta1}\cos\varphi_s \quad (26)$$

Then, the current equations of the IM2:

$$i_{m2\alpha2} + i_{ir2\alpha2} = i_{s2\alpha2} + i_{r\alpha1}\cos\varphi_s + i_{r\beta1}\sin\varphi_s \quad (27)$$

$$i_{m2\beta2} + i_{ir2\beta2} = i_{s2\beta2} - i_{r\alpha1}\sin\varphi_s + i_{r\beta1}\cos\varphi_s \quad (28)$$

The implementation of equations of (13)-(28) allow us to calculate all needed currents and flux linkages in the stationary frames linked to two stators. The stator and iron losses currents and magnetizing flux linkage of the IM2 are obtained in the frame of α2β2 but to transform it to α1β1 should not be an issue. Also, it should be noticed that the stator rotation speed of $\omega_s$ is much smaller than the rotors speed of $\omega_r$. As a result, all components of equations of (15)-(18) and (21), (22), contenting of $\omega_s$, become neglectable.

The general expression for torque of an induction motor:

$$T_e = \frac{1}{2}\frac{\partial}{\partial\varphi_s}\sum_{n=s1\alpha1}^{r2\beta2} i_n\lambda_n = \frac{1}{2}\sum_{n=s1\alpha1}^{r2\beta2} i_n\frac{\partial\lambda_n}{\partial\varphi_s} \quad (29)$$

The torque is the result of interaction of magnetically coupled inductances. For the IM1 all inductances place ortgonal axes while inductances of the IM2 place on axes mutual position of that depend on rotation angle of $\varphi_s$. The expression for torque of each induction motor:

$$T_{e1} = \frac{3}{2}\frac{p_n}{L_{lr}}\left[\left(L_{lr}i_{r\alpha1} + \lambda_{\mu1\alpha1}\right)\lambda_{\mu1\beta1} - \left(L_{lr}i_{r\beta1} + \lambda_{\mu1\beta1}\right)\lambda_{\mu1\alpha1}\right]$$

$$T_{e2} = \frac{3}{2}\frac{p_n}{L_{lr}}\left[\left(L_{lr}i_{r\alpha1} - \lambda_{m2\alpha2}\cos\varphi_s + \lambda_{m2\beta2}\sin\varphi_s\right)\times\right.$$

$$\times\left(-\lambda_{m2\alpha2}\sin\varphi_s - \lambda_{m2\beta2}\cos\varphi_s\right) + \left(L_{lr}i_{r\beta1} - \lambda_{m2\alpha2}\sin\varphi_s -\right.$$

$$\left.\left. - \lambda_{m2\beta2}\cos\varphi_s\right)\left(-\lambda_{m2\alpha2}\cos\varphi_s + \lambda_{m2\beta2}\sin\varphi_s\right)\right]$$

The total torque of both IM1 and IM2:

$$T_{e\Sigma} = T_{e1} + T_{e2} \quad (30)$$

The induction motor with rotatory stator is an electric motor having two moving units which are stator and rotor. Thus, the equations of mechanic moving are the next:

$$\frac{J_{r\Sigma}}{p_n}\frac{d\omega_r}{dt} = T_{e\Sigma} - T_L \quad (31)$$

$$\frac{J_{s\Sigma}}{p_n}\frac{d\omega_s}{dt} = T_{e2} - T_{Ls} \quad (32)$$

where $J_{s\Sigma}$, $J_{r\Sigma}$ denote the total moments of inertia of the rotatory stator of IM2 and the rotor shafts of IM1 and IM2 with the mechanical units coupled to them, respectively, $p_n$ denotes the number of the stator winding pole pairs, $T_{Ls}$, $T_L$ denote the load torque applied to the rotatory stator and the rotor shafts, respectively.

## 4. Results of simulation

Simulation of the electric drive was carried out by using of Matlab.

The load device in simulation was a centrifugal fan with square dependence of load torque from speed. The rated parameters of induction motors of IM1 and IM2 are the next: $P_{rat}$= 2.2 kW, $V_{s,rat}$=220 V, $f_{s,rat}$=50 Hz, $p_n$=3, $R_s$=3.6 Ω, $R_r$=4.19 Ω, $L_{ls}$=0.0082 Hn, $L_{lr}$=0.0116 Hn, $L_m$=0.1 Hn, $R_{ir}$=1432 Ω, where $P_{rat}$, $V_{s,rat}$ and $f_{s,rat}$ denote the output power, stator voltage and its frequency, respectively.

The simulation was replicated with the stator current frequency of $f_s \le 50$ *Hz*.

The dependance of the $R_{ir}$ from the $f_s$ was taken into account by the next emprical equation [7]:

$$R_{ir} = 250.49 + 16.02 f_s + 0.152 f_s^2$$

The dependance of the $L_m$ from the magnetising current, $I_m$, was taken into account by the next equation [7]:

$$L_{m*} = -0.002I_{m*}^6 + 0.037I_{m*}^5 - 0.261I_{m*}^4 + 0.87I_{m*}^3 -$$

$$-1.287I_{m*}^2 + 0.214I_{m*} + 1.413$$

where

$$L_{m*} = L_m / L_{m,rat},\ I_{m*} = I_m / I_{m,rat}$$

Some results of simulation are shown in Fig. 5, 6.

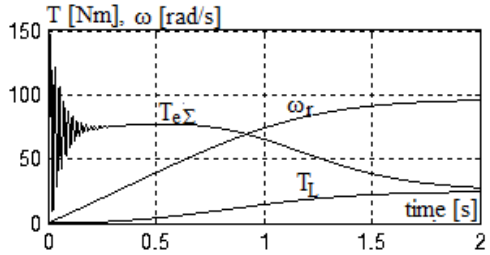


a

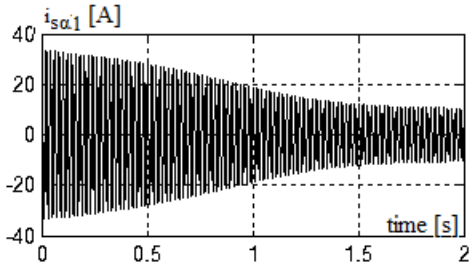


b

Fig. 5. Results of simulation
($V_s$ = 220 *V*, $f_s$ = 50 *Hz*, $\varphi_s = \pi$ *rad*)

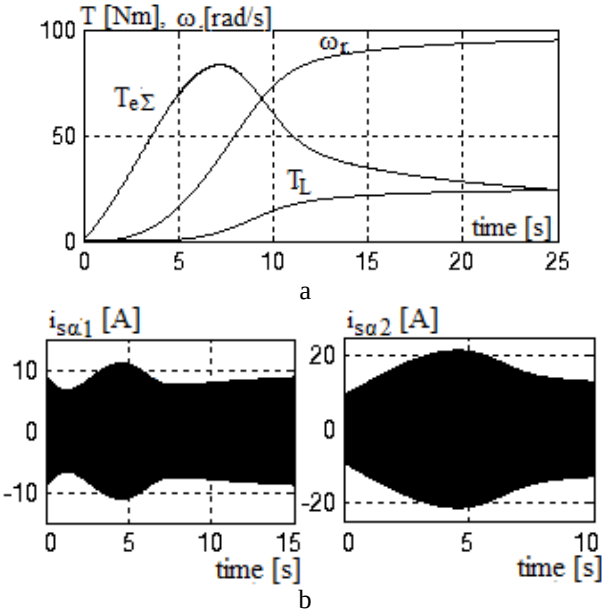


Fig. 6. Results of simulation

($V_s$ = 220 *V*, $f_s$ = 50 *Hz*, $\varphi_s = \begin{cases} \pi t / 20\, rad, t \le 20s \\ \pi\, rad, t > 20s \end{cases}$)

As it could be seen from Fig. 5 and 6, the soft changing of $\varphi_s$ from *0* to $\pi$ leads to decreasing of total stator current and torque. It should be noticed that the $\varphi_s = \pi$ provides the equality of the stator currents of both IM1 and IM2. While $\varphi_s = 0$, the stator currents also equal to each other and roughly to no-load current. While $0 < \varphi_s < \pi$, the stator currents have different values.

Also, the results of simulation show that even for zero angle between the two stators there is quite a high value of the short-term peak transient stator current due to switching of the stator windings, i.e. RL circuit, to the full voltage of the grid. This peak value is restricted only by the stator resistance, electrical inertia of the stator inductance and level of the magnetic saturation, so for the stronger restriction of the transient currents it could be recommended to put a short-duty resistance series to the stator winding. Another way to avoid the high peak current is to employ a synchronous generator that diminishes the current due to its own reactance (synchronous generator is also used for the experimental investigations in the next Section). This is feasible especially for vehicles that supply all electrical loads by a generator. It should be noticed that the ratio of the peak current to the rated one increases with increasing of the power of electric drive. For a small and medium power drives (no more than a few tens of kW), the peak value of the current does not exceed 1.5...2.0 the rated current and does not lead to any dangerous consequences. Thus, the problem of the peak current needs careful consideration for the large drives where employment of the additional short-duty devices or synchronous generator could reduce the peak current and provide desirable soft start.

## 5. Experimental setup and results

The performance of the suggested electric drive is experimentally validated by results obtained by experimental setup, the block diagram of which shown in Fig.1. The experimental setup itself is shown in Fig. 7.

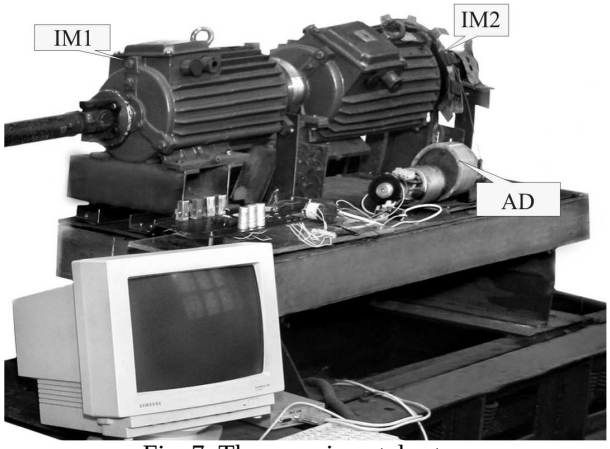


Fig. 7. The experimental setup

The details of IM1 and IM2 connections are described in Section 2, the parameters of the induction motors are presented in Section 4. After survey being carried out, the DC motor fed by IGBT-based H-bridge circuit is decided to be used as the auxiliry device, AD, for the purpose of rotation of the IM2 stator. The DC motor speed and angle is controlled by means of pulse-width modulation of the armature voltage. The power of DC motor has to be enough to rotate the IM2 stator and hold it in the position needed. The load torque of the DC motor is the torque of the IM2, $T_{e2}$. The transfer unit between the DC motor and the stator is a worm reduction unit linked to the stator by steel rope. The rated electrical parameters of the DC motor are the follows: the armature voltage is 220 V, the armature current is 1.1 A.

The centrifugal fan coupled to the IM1 and IM2 shafts by cardan shaft is the load device of the electric drive.

ACS712 current sensors, manufactured by Allegro Microsystems, are used for current measurement. E40S6 incremental encoders, manufactured by Autonics, are used for the IM1 and IM2 rotors speed and DC motor speed and angle measurements.The signals from all current sensors and encoder are connected to the multi-function board of analog-to-digital conversion of the LA-2USB, manufactured by Rudnev-Shilyaev, and from it to the personal computer.

The stator windings of the IM1 and IM2 are supplied by voltage coming from synhcronous generator that provide its sinusoidal shape and, as it was stressed before in Section 4, reducing of the peak transient current.

Fig. 8 and 9 show the both experimental and simulation results.

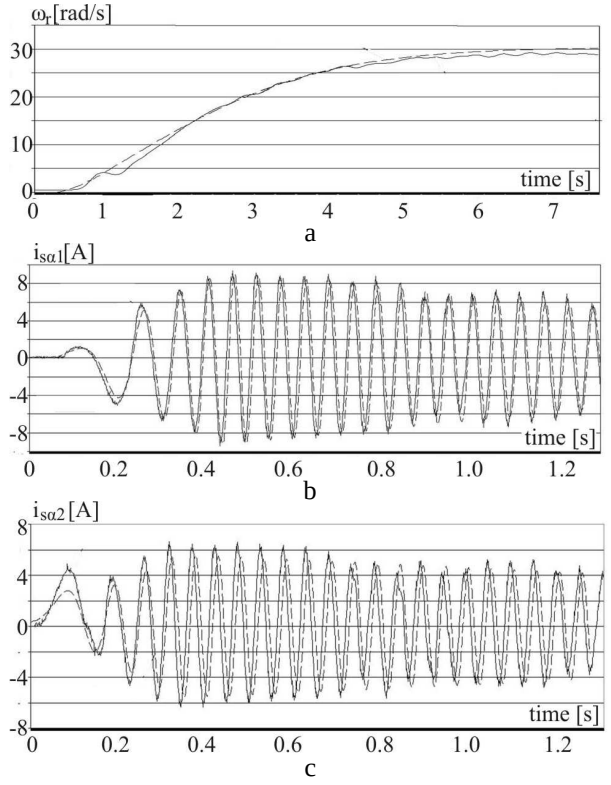


Fig. 8. Results of experimental (solid) and simulation (dashed) investigation of transient mode ($V_s$ = 50 *V*, $f_s$ = 17.5 *Hz*, $\varphi_s = \pi/2$ *rad*)

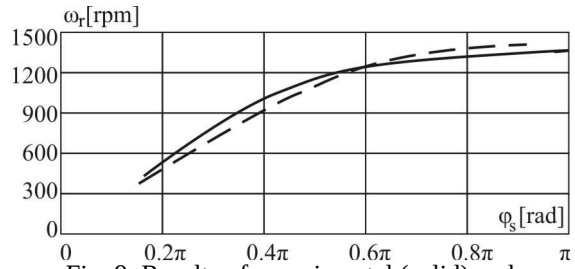


Fig. 9. Results of experimental (solid) and simulation (dashed) investigation of steady state ($V_s$ = 220 *V*, $f_s$ = 50 *Hz*)

## 6. Assessment of efficiency

As it could be seen from the Fig. 9, two induction motors electric drive has an ability to control speed over some range. It indicates to the fact that this electric drive could be implemented not only as soft-starter but also as an adjustable drive. To assess this possibility, it needs to calculate the feasible range of speed in which the electric drive has the appropriate efficiency and power losses. The next equations were employed to estimate the power losses.

The mechanical power on the motor shaft:

$$P_{mech} = T_{e\Sigma}\omega_r / p_n \tag{33}$$

The active electric power of each motor:

$$P_{s1} = \frac{3}{2}\left(i_{s1\alpha1}u_{s1\alpha1} + i_{s1\beta1}u_{s1\beta1}\right) \tag{34}$$

$$P_{s2} = \frac{3}{2}\left(i_{s2\alpha2}u_{s2\alpha2} + i_{s2\beta2}u_{s2\beta2}\right) \tag{35}$$

The total active electric power of the electric drive:

$$P_{s\Sigma} = P_{s1} + P_{s2} \tag{36}$$

According to the Fig. 3, the total power losses of the electric drive consist of losses in the copper of the two stator windings and two rotor windings and losses in the iron of the two stator yokes. The total power losses can be found from the equation of power balance:

$$P_{loss} = P_{s\Sigma} - P_{mech} \tag{37}$$

The dependence of ratio of the total power losses to the rated mechanical power of the electric drive, $P_{rat,\Sigma} = P_{rat,1} + P_{rat,2} = 2P_{rat}$, from the rotation angle is shown in Fig. 10.

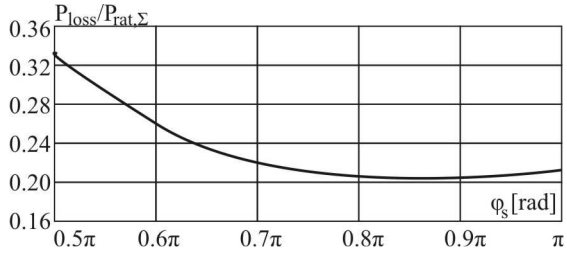


Fig. 10. Ratio of the power losses to the rated power vs. rotation angle ($V_s$ = 220 *V*, $f_s$ = 50 *Hz*)

It should be noticed that, with the $\varphi_s=\pi$, the power losses coincide with its rated value. As it could be seen from the Fig. 10, the curve of the power losses has the clear point of minimum with values of the rotation angle smaller than $\pi$ (this case $\varphi_s=0.86\pi$). Since the difference of speed caused by changing of $\varphi_s$ from $\pi$ to $0.86\pi$ is very small (Fig. 9) then it could be recommended to adjust the rotation angle in the position that provides the minimum of losses. The considerable decrease of the $\varphi_s$ leads to excessive raising of the losses.

So, besides the soft start, implementation of two induction motors electric drive gives the other important advantage that is ability to vary speed in a small range leading to the reduction of power losses with shifting angle $\varphi_s$.

## 7. Approximate comparative assessment of the electric drives

Introducing of the new kind of electric drive or the new technique of soft start/stop requires some economic calculations to prove its practical feasibility. Based on survey of Internet resources, the Table 1 summarizes the cost of the clue equipments of electric drives. The observed frequency converters provide *V/f* and some kind of vector controls, the soft starters are based on semiconductor devices and provide the soft start and stop. The both converter and starter have enclosure rating IP20. The induction motors are totally enclosed fan cooled (TEFC) squirrel cage foot mounted ones.

Table 1
Comparative assessment of equipments of the different electric drives

| Equipment | Frequency converter | | | Soft starter | | | Induction motor | | |
|---|---|---|---|---|---|---|---|---|---|
| Power | 7.5 kW | 55 kW | 110 kW | 7.5 kW | 55 kW | 110 kW | 7.5 kW | 55 kW | 110 kW |
| Price, $ | 400... 470 | 2600... 3000 | 4700... 5400 | 350... 400 | 580... 650 | 1300... 1500 | 280... 330 | 1050... 1150 | 2000... 2200 |

To calculate approximately cost of the whole drive, it needs to add the price of an induction motor and price of frequency converter or soft starter depending on the type of electric drive.

The cost of the two induction motors electric drive is determined mostly by the price of the two TEFC slipring motors with the halved power of each one. Price of the two motors is 490...540$ for the 7 kW (2 x 3.5 kW), 1500...1600$ for the 60 kW (2 x 30 kW), 2450...2700$ for the 110 kW (2 x 55 kW). The all considered motors have 4 poles. The cost of additional device to rotate the stator depends on the type of this device. The servo drive with AC or DC brushless motor is recommended to be used. Its power determines the cost and the speed of the stator rotation. Generally, the power of servo motor is the next:

$$P_{ad} = T_{e2}\omega_s = T_{e2} d\varphi_s / dt \quad (38)$$

The more power, the higher speed of the stator rotation and the faster torque response of the whole drive could be delivered. The range of geometrical angle of rotation for the 4 pole motor is $\varphi_s=\pi/2$. Thus, servo drive has to give the minimal transient time of this small rotation. It should be noticed that for the fans there are no strong requirements on the fast torque response and transient modes so the servo drive could be chosen for the transient time of the stator rotation of at least a few seconds to provide soft start, stop and the speed varying in the small range. The holding of the stator in the still position during steady state could be done by worm gear box reduction or any mechanical brake presenting the main components of transmission between the servo motor and the stator. The calculations of equation (38) show that the output torque of transmission varies about 20 to 365 Nm for the two 3.0...55 kW 4 pole motors. The power of servo drive (without power losses in the transmission) for the 5 sec transient time is 6.28...115 W. So, the power and energy consumptions of servo drive could be neglected relatively to the power of the whole drive. The cost of brushless servo drive with position control for the considered range of power is 200...500$. The cost of transmission is 100...250$.

So, the total cost of the proposed electric drive varies 800...1000$ for the 7.5 kW to 3200...3450$ for the 110 kW. Analyzing the Table1 allows to conclude that relevance of the two induction motors electric drive increases with increasing power of drive. It has fewer cost relatively to frequency converter - induction motor drive and comparable cost to semiconductor soft starter - induction motor drive since a few tens of kW.

## 8. Conclusion

The electric drive proposed in this article has the two identical slipring induction motors one of which has rotatory stator that allows to restrict the start current. The electric drive requires more complicated mechanical mounting than the industrial ones but it does not have any semiconductors in the stator or rotor circuits. The problem of the short-term peak transient current appearing for the large drives could be solving by putting the short-duty series resistances or supplying from synchronous generator as it happens on vehicles. The great advantage of the considered drive before the industrial soft starters is ability to vary speed in a small range leading to the reduction of power losses with shifting angle of rotation. The torque response is quite a slow and depends on power of servo drive rotating the stator. The electric drive is appropriate for the fans where there is no strong requirement on transient time. The electric drive has economic gain on its cost before inverter fed motor since a few tens of kW.

**References**


1. Thanga Raj, C, Srivastava, S.P,. Agarwal, P. *Energy efficient control of three-phase induction motor - a review*. In: International Journal of Computer and Electrical Engineering, Vol. 1, No. 1, April 2009. p. 61 – 70.
2. Thorsen, O.V., Dalva, M. *A survey of the reliability with an analasis of faults on variable frequency drives with in industry*. In: EPE'95, Spain, 1995, p. 1033 – 1038.
3. Abdel-Halim, Fiet, A.M., Al-Ahmar, M.A., Elfaraskoury, M.E., Mahmoud E.M. *A novel approach for the analysis of a thyristor- controlled induction motor*. In: Journal of Electrical Engineering, Vol. 15, 2015, Edition 2, p. 101 – 112.
4. Siddiqui, U.F., Verma, A., Soni, S. *Comparative Performance Analysis of Induction Motor Using Semiconductor Devices in Terms of Firing Angle*. In: International Journal of Emerging Technology and Advanced Engineering, Vol 4, Issue 2, February, 2014, p. 280 – 285
5. Riyaz, A., Iqbal, A., Moinoddin, S., MoinAhmed, S., Abu-Rub, H. *Comparative performance analysis of Thyristor and IGBT based induction motor soft starters*. In: International Journal of Engineering, Science and Technology, Vol. 1, No. 1, 2009, p. 90 – 105.
6. Nowotny, D., Lipo, T. *Vector Control and Dynamics of AC drives.* Clarendon Press, Oxford, UK, 1996.
7. Kosmodamianskii, A.S., Klyachko L.M., Vorobiev V.I., Pugachev, A.A. *Control system of a tractive drive with temperature control of thermally loaded elements*. In: Russian Electrical Engineering, Vol. 85, No. 8, 2014, p. 513 – 518.